Cell Death and Differentiation (2016) 23, 29–40

www.nature.com/cdd

Intracellular nicotinamide adenine dinucleotide promotes TNF-induced necroptosis in a sirtuin-dependent manner

N Preyat[1], M Rossi[2], J Kers[3], L Chen[4], J Bertin[5], PJ Gough[5], A Le Moine[2], A Rongvaux[6], F Van Gool[7] and O Leo[*,1,2]

Cellular necrosis has long been regarded as an incidental and uncontrolled form of cell death. However, a regulated form of cell death termed necroptosis has been identified recently. Necroptosis can be induced by extracellular cytokines, pathogens and several pharmacological compounds, which share the property of triggering the formation of a RIPK3-containing molecular complex supporting cell death. Of interest, most ligands known to induce necroptosis (including notably TNF and FASL) can also promote apoptosis, and the mechanisms regulating the decision of cells to commit to one form of cell death or the other are still poorly defined. We demonstrate herein that intracellular nicotinamide adenine dinucleotide (NAD^+) has an important role in supporting cell progression to necroptosis. Using a panel of pharmacological and genetic approaches, we show that intracellular NAD^+ promotes necroptosis of the L929 cell line in response to TNF. Use of a pan-sirtuin inhibitor and shRNA-mediated protein knockdown led us to uncover a role for the NAD^+-dependent family of sirtuins, and in particular for SIRT2 and SIRT5, in the regulation of the necroptotic cell death program. Thus, and in contrast to a generally held view, intracellular NAD^+ does not represent a universal pro-survival factor, but rather acts as a key metabolite regulating the choice of cell demise in response to both intrinsic and extrinsic factors.

Cell Death and Differentiation (2016) **23,** 29–40; doi:10.1038/cdd.2015.60; published online 22 May 2015

Nicotinamide adenine dinucleotide (NAD^+) has been long recognized as a key intermediate in cellular metabolism. By accepting and donating electrons in reactions catalyzed by dehydrogenases, NAD^+ has, for example, a central role in the generation of ATP, a molecule required for most energy-consuming cellular reactions. The recognition of NAD^+ as a substrate in a number of regulatory processes has shed a new light on its role in cell physiology. Indeed, NAD^+ represents a substrate for a wide range of enzymes including cADP-ribose synthases, poly (ADP-ribose) polymerases (PARPs) and the sirtuin family of NAD^+-dependent deacylases (SIRTs). In marked contrast to its role in energy metabolism, the involvement of NAD^+ in these enzymatic reactions is based on its ability to function as a donor of ADP-ribose, a reaction that, if sustained, can lead to the depletion of the intracellular NAD^+ pool.[1–5]

The pro-survival role of NAD^+ has been particularly well described in cells exposed to genotoxic/oxidative stress. In response to DNA damage, PARP1, the founding and most abundant member of the PARP family, binds to DNA strand breaks and initiates a repair response by catalyzing the post-translational modification of several nuclear proteins, including itself. This protective response is characterized by the transfer of successive units of the ADP-ribose moiety (up to 200 units) from NAD^+ to other proteins, compromising therefore both energy production (slowing the rate of glycolysis, electron transport and ATP formation) and activity of other NAD^+-dependent enzymes through NAD^+ depletion.[6,7] Moreover, PARP1-synthesized PAR polymers can be degraded into free oligomers, known to translocate to the mitochondria where they can trigger the release of AIF from mitochondria to the nucleus.[8–11] The precise molecular steps linking PARP1 activation to this form of stress-induced cell death, termed parthanatos, have not been fully elucidated, and probably depend on the particular metabolic status of the cell examined (i.e., anerobic glycolysis in most *in vitro* cell lines *versus* oxidative metabolism of neuronal cells, see Welsby *et al.*[12] for review). In any instances, and independently of the fine

[1]Laboratory of Immunobiology, Institute for Molecular Biology and Medicine, Université Libre de Bruxelles, Gosselies, Belgium; [2]Institute for Medical Immunology, Université Libre de Bruxelles, Gosselies, Belgium; [3]Department of Pathology, Academic Medical Center, University of Amsterdam, Amsterdam, The Netherlands; [4]Center for Drug Design, Academic Health Center, University of Minnesota, Minneapolis, MN 55455, USA; [5]Pattern Recognition Receptor Discovery Performance Unit, Immuno-Inflammation Therapeutic Area, GlaxoSmithKline, Collegeville, PA 19426, USA; [6]Department of Immunobiology, Yale University School of Medicine, New Haven, CT, USA and [7]Diabetes Center, University of California San Francisco, San Francisco, CA, USA

*Corresponding author: O Leo, Laboratory of Immunobiology, Institute for Molecular Biology and Medicine, Université Libre de Bruxelles, Rue des Profs Jeener et Brachet 12, Gosselies 6041, Belgium. Tel: +3226509877; Fax: +3226509860; E-mail: oleo@ulb.ac.be

Abbreviations: ADP, adenosine-5'-diphosphate; AIF, apoptosis-inducing factor; ATP, adenosine-5'-triphosphate; FLIP, FLICE inhibitory protein; CRISPR, Clustered Regularly Interspaced Short Palindromic Repeats; CCL2, chemokine (C-C motif) ligand 2; CXCL1/2, chemokine (C-X-C motif) ligand 1/2; CrmA, cytokine response modifier A; DNA, deoxyribonucleic acid; GM-CSF, granulocyte-macrophage colony-stimulating factor; IκBαSR, inhibitor of nuclear factor kappa B alpha super repressor; IL-6/8/1β, Interleukin-6/8/1β; iNam, isonicotinamide; JNK, c-Jun N-terminal kinases; MLKL, mixed lineage kinase domain-like; MNNG, methyl-N'-nitro-N-nitrosoguanidine; NAD, nicotinamide adenine dinucleotide; NAMPT, nicotinamide phosphoribosyl tranferase; NF-κB, nuclear factor kappa B; NMN, nicotinamide mononucleotide; PAR, poly ADP-ribose; PARP, poly (ADP-ribose) polymerase; RIPK1/3, receptor interacting serine-threonine kinase 1/3; RNA, ribonucleic acid; shRNA, short hairpin RNA; siRNA, small interfering RNA; SDS, Sodium dodecyl sulfate; SMAC, second mitochondria-derived activator of caspases; TNF, tumor necrosis factor; TNFR1, TNF receptor 1

Received 17.1.14; revised 16.4.15; accepted 20.4.15; Edited by P Vandenabeele; published online 22.5.15

molecular events at work, virtually all studies have identified the brisk loss of intracellular NAD^+ as the critical step initiating this specific form of cell death. The protective role of NAD^+ in PARP1-dependent cell death has been indeed amply documented.[13–18] In mammals, nicotinamide (Nam) acts as the main precursor for NAD^+ biosynthesis and nicotinamide phosphoribosyl tranferase (NAMPT) is the rate-limiting enzyme for NAD^+ biosynthesis from Nam.[19] *Nampt* deficiency in mice leads to lethality and the heterozygous animals suffer from significant perturbations related to their NAD^+ metabolism.[20] In keeping with the general role of NAD^+ as a survival factor in cells exposed to genotoxic stress, genetic ablation of *Nampt* and/or treatment with a specific NAMPT inhibitor (FK866) sensitized cells to the toxic effects of alkylating agents.[16,18] Similarly, overexpression of a catalytically active recombinant NAMPT protected the NIH-3T3 cell line from the toxicity of the same DNA alkylating agents,[18] further establishing a functional link between NAD^+ biosynthesis and sensitivity to stress-induced, PARP1-dependent cell death.

While analyzing the influence of NAD metabolism on survival of NIH3T3 cells exposed to genotoxic agents, we observed that overexpression of NAMPT prolonged cell survival of cells exposed to the alkylating agent N-methyl-N'-nitro-N-nitrosoguanidine (MNNG), and unexpectedly, led to increased sensitivity to cell death induced by the pro-inflammatory cytokine TNF.[18] TNF is a pleiotropic cytokine regulating many cellular functions and known to induce several forms of cell death, including apoptosis and the recently uncovered regulated form of necrosis termed necroptosis.[21,22] In contrast to apoptosis, necroptosis is largely independent of the so-called executioner caspase (such as caspase-3, 6 and 7) activity and is initiated by the formation of a signaling complex comprising the receptor-interacting serine-threonine kinase 1 (RIPK1), RIPK3 and the recently identified mixed lineage kinase domain-like protein MLKL. Although necroptosis often appears to occur when apoptosis is abortive (such as in situations of caspase inhibition), the cellular factors regulating the choice between these two forms of regulated cell death have not been fully uncovered. Using a model cell line engineered to respond to both apoptosis and necroptosis, we demonstrate herein that intracellular NAD^+ represents a critical factor in promoting cell death by necroptosis. In keeping with the well-described role of sirtuins as intracellular NAD^+ sensors, we also demonstrate that sirtuins, and in particular SIRT2 and SIRT5, are required for adequate completion of the necroptotic program in response to TNF. Accordingly, a pan-sirtuin inhibitor was found to attenuate organ damage induced by transient ischemia. Thus, intracellular NAD^+, rather than acting as a general cell survival factor, appears to promote cell necroptosis in a sirtuin-dependent manner, a finding that may suggest novel therapeutic approaches to attenuate *in vivo* necrotic insults in several pathological settings.

Results

Intracellular NAD^+ promotes necroptosis. To evaluate the role of intracellular NAD^+ in regulating cell sensitivity to cell death, we took advantage of the cellular subline L929sAhFAS (referred hereafter to as L929), generated by stable transfection of the murine fibrosarcoma L929sA cell line with the human pro-apoptotic receptor hFAS.[23] The L929 cell line undergoes apoptotic cell death in response to agonistic anti-hFAS antibodies, while dying by necroptosis when incubated in the presence of recombinant murine (mTNF) or human TNF (hTNF). The advantage of this model is that necroptosis and apoptosis can be induced in the absence of pharmacological inhibitors (such as SMAC mimetics, protein synthesis or caspase inhibitors) that could complicate interpretation of the mechanisms at work. To evaluate the role of intracellular NAD^+ in controlling L929 response to FAS and TNF, cells were incubated in the presence of the potent NAMPT inhibitor FK866. Target specificity of FK866 was ascertained by addition of nicotinamide mononucleotide (NMN), the product of the NAMPT-catalyzed reaction, to the culture media. As shown in Figure 1a, cell exposed to FK866 displayed a substantial reduction in intracellular NAD^+ levels (in excess of 75%), readily reverted by simultaneous addition of NMN. NAD^+-deprived cells were found to display increased sensitivity to hFAS-induced apoptosis (Figure 1b), while resisting the cell death-inducing activity of hTNF (Figure 1c). In keeping with its NAD^+ restoring properties shown in Figure 1a, NMN reestablished the original sensitivity of L929 cells to cell death-inducing agents (Figures 1b and c). To confirm that adequate intracellular NAD^+ levels are required for TNF-induced cell death in the L929 cell line, cells were treated by the synergistic combination of siRNA to Nampt and low doses of FK866, a treatment previously shown to reduce intracellular NAD^+ with minimal cell toxicity.[16,24] In agreement with the previous observations, this treatment led to a significant protection against TNF-induced cell death (Figure 1d). Finally, two alternative and independent pharmacological approaches were used to demonstrate the positive correlation between high intracellular NAD^+ levels and sensitivity to mTNF-induced necroptosis. Isonicotinamide (iNam) is an isomer of nicotinamide recently shown to cause intracellular NAD^+ accumulation in both yeast and human cells.[25] L929 cells incubated in the presence of iNam displayed increased sensitivity to necroptosis that was readily reverted in the presence of necrostatin-1 (Figure 1e). Note that iNam was not toxic when added to the media, and even slightly protected cells against hFAS-induced cell death (Figure 1e). In keeping with the well-established protective role of NAD^+ against genotoxic/oxidative insults, iNam inhibited L929 cell necrosis induced by a genotoxic agent (MNNG) known to cause PARP1-dependent necrosis (Figure 1f). Of particular interest, iNam sensitized murine embryonic fibroblasts (MEFs) to TNF-induced necroptosis, a form of cell death inhibited by both necrostatin-1 (Figure 1g) and a recently developed specific inhibitor of the kinase activity of RIPK3 (R3i)[26,27] (Supplementary Figure S1), further confirming that independently of the experimental strategy used, intracellular NAD^+ appears to promote necroptotic cell death. Finally, we examined the capacity of RIPK3 to be recruited into RIPK1-containing complexes upon TNF stimulation. As shown in Figure 1h, TNF induced assembly of RIPK1-RIPK3 complexes in control, but not in FK866-exposed cells, suggesting

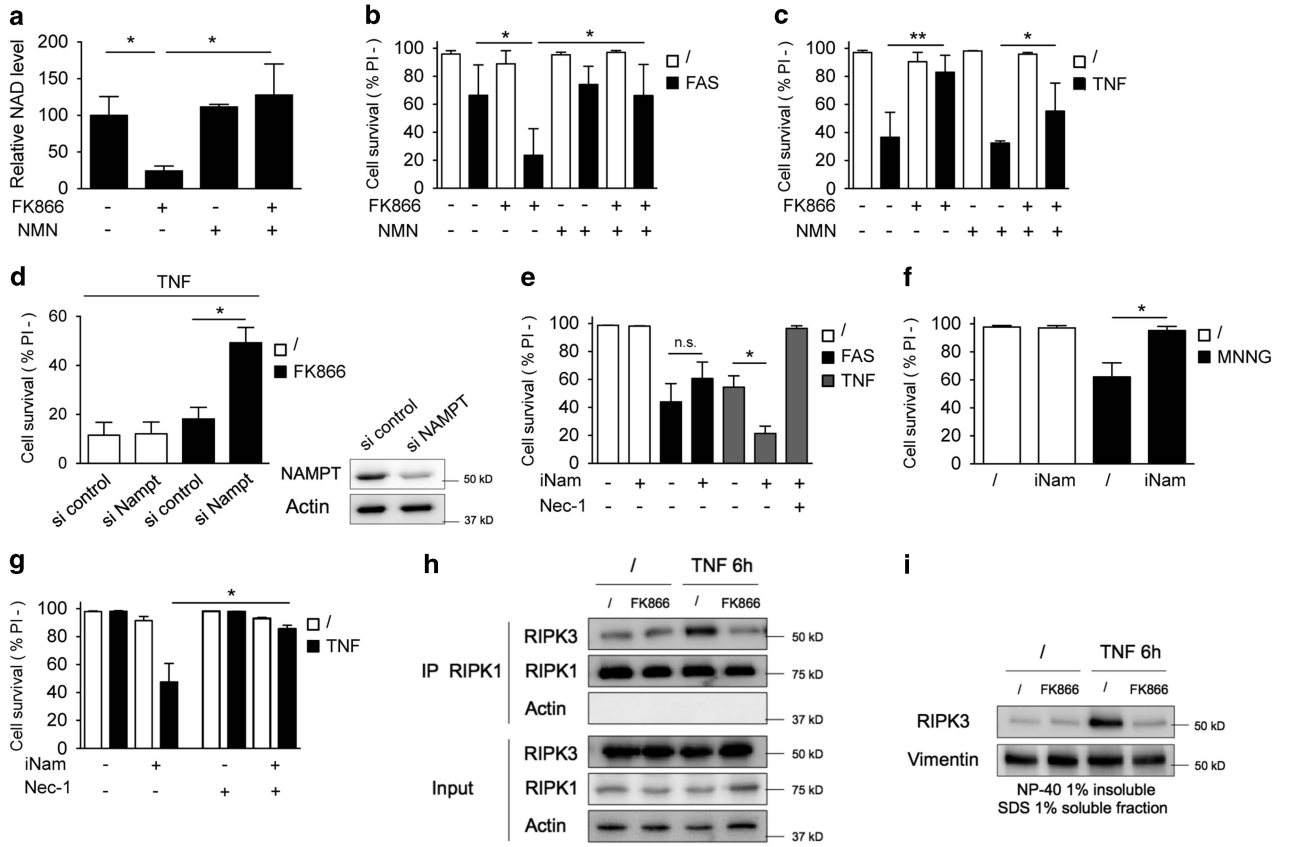

Figure 1 Intracellular NAD^+ promotes TNF-induced necroptosis. (**a**) L929 cells were incubated in the presence of 100 nM of FK866, 5 mM of nicotinamide mononucleotide (NMN) and a combination of both compounds, and total NAD levels determined as described in the Methods section ($n=4$). (**b**, **c**) L929 cells cultured as in (**a**) were further incubated in the presence of (**b**) anti-hFAS-activating antibodies (clone CH-11; 50 ng/ml) ($n=6$) or (**c**) recombinant hTNF (1 ng/ml) ($n=6$). Cell survival at 16 h post-treatment was monitored by flow cytometry. (**d**) Control and NAMPT siRNAs-treated L929 cells were incubated or not in the presence of 10 nM of FK866, followed by hTNF (1 ng/ml) ($n=4$). Western blot analysis was used to evaluate the efficacy of NAMPT siRNAs on NAMPT protein expression ($n=2$). (**e**) Cell survival in response to FAS (CH-11)-induced apoptosis or TNF-induced necroptosis was assessed in cells previously incubated in the presence of 10 mM of isonicotinamide (iNam) for 8 h. Necrostatin-1 (Nec-1) was used to confirm necroptotic death in response to TNF+iNam (10 mM) ($n=4$). (**f**) L929 cells were incubated in the presence of iNam (10 mM) for 8 h, then treated with MNNG (600 μM) as indicated and cell survival at 16 h post-treatment was monitored by flow cytometry ($n=4$). (**g**) MEFs were incubated in the presence of iNam (40 mM) for 8 h, exposed to hTNF (1 ng/ml) for 16 h before monitoring cell survival. (**h**) FK866 (100 nM)-treated L929 cells were stimulated with hTNF for 6 h, and cell extracts analyzed for the presence of RIPK1-RIPK3 protein complexes using immunoprecipitation with an anti-RIPK1 antibody and western blot analysis with an anti-RIPK3 probe ($n=3$). (**i**) FK866 (100 nM)-treated L929 cells were stimulated with hTNF for 6 h and the NP-40 1% insoluble fraction analyzed by western blotting for the presence of RIPK3 ($n=3$). Data represent mean+SD of at least three independent experiments (*$P<0.05$, **$P<0.01$)

a critical role for intracellular NAD^+ in mediating early signaling to necroptosis. Furthermore, RIPK3 was found associated to a NP-40 1% insoluble/SDS 1% soluble fraction after TNF treatment only in control but not in FK866-treated cells (Figure 1i), compatible with the previously described accumulation of RIPK3 to a membrane fraction insoluble to mild detergents.[28–31]

A pan-sirtuin inhibitor protects cells from necroptosis. The enzymatic activity of members of the sirtuin family of NAD^+-dependent deacetylases has been shown to require adequate intracellular NAD^+ level.[32] We therefore postulated that one or several members of this family might be involved in the signaling pathway leading to necroptosis, an hypothesis recently suggested by an independent study.[33] Three structurally unrelated sirtuin inhibitors (EX-527,[34] compound 64[35] and cambinol[36]) protected L929 cells from TNF-induced cell death (Figures 2a–c, see also Supplementary Figure S2 for a typical flow cytometry data plot). Cambinol was selected for further characterization throughout this study and shown to selectively protect L929 cells from TNF-induced necroptosis (Figure 2e) but not FAS-dependent apoptosis (Figure 2d). Necrostatin-1 was used herein as a further confirmation of the necroptotic cell death in response to TNF (Figures 2d and e). We also noticed that cambinol and necrostatin-1 displayed additive effects when added simultaneously to L929 cells, raising the possibility that these compounds may affect distinct steps of the TNFR1 signaling cascade (Supplementary Figure S3a). Note that in addition to promote FAS-induced apoptosis (Figure 2d), cambinol also sensitized cells against ionomycin-induced cell death (Supplementary Figure S3b), further illustrating the fact that this compound does not act as a non-specific, life-preserving agent. Finally, incubation of L929 cells in the presence of cambinol led to the accumulation of acetylated forms of tubulin, a well-characterized SIRT2 substrate, in keeping with its sirtuin

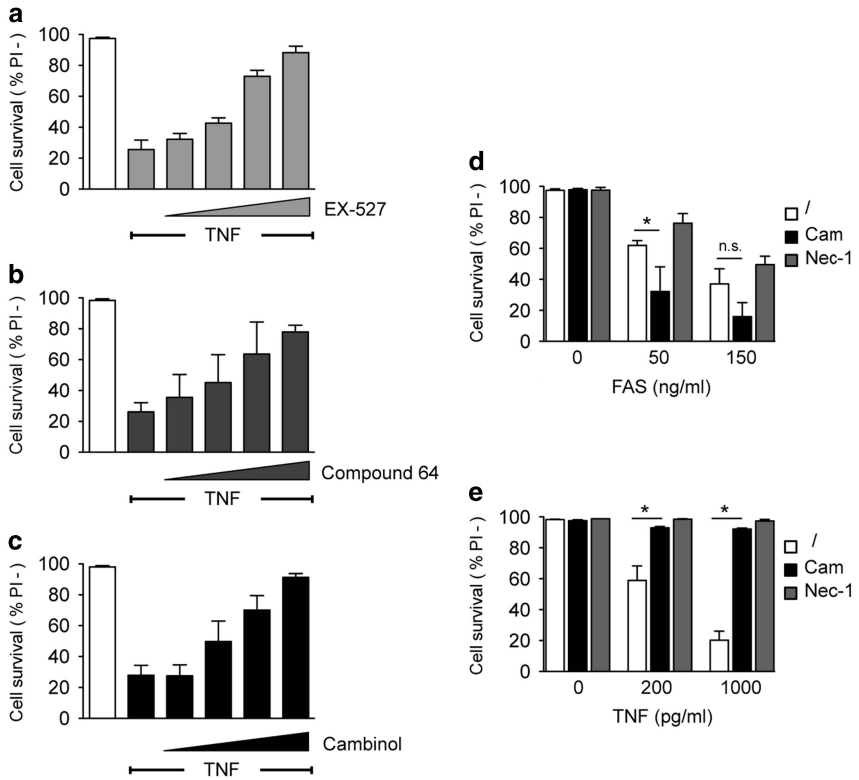

Figure 2 Sirtuin inhibitors protect from TNF-induced necroptosis but not FAS-mediated apoptosis. (**a**–**c**) Cell survival in response to recombinant hTNF (1 ng/ml)-induced necroptosis was assessed 16 h post-treatment in L929 cells previously incubated in the presence of increasing doses of (**a**) EX-527 ($n=4$) (**b**) compound 64 ($n=4$) and (**c**) cambinol ($n=4$). A maximum dose of 200 μM was used for all inhibitors. Three-fold serial dilutions were used for cambinol and two-fold serial dilutions were used for EX-527 and compound 64. (**d**, **e**) L929 cells were incubated in the presence of cambinol (100 μM) or necrostatin-1 (20 μM) and cell death induced by anti-hFAS ($n=4$) (**d**) or hTNF ($n=4$) (**e**). Data represent mean+SD of four independent experiments (*$P<0.05$)

inhibiting properties (Supplementary Figure S3c). A series of experiments was conducted to firmly exclude that the protective role of cambinol was related to its capacity to alter the expression of a NF-κB-dependent survival gene. Cambinol protected cells from necroptosis even in the presence of the protein synthesis inhibitor cycloheximide (Figure 3a). Cambinol displayed a weak, but reproducible inhibitory effect on TNF-induced NF-kB signaling (Figure 3b). Cells overexpressing the specific and potent NF-κB inhibitor IκBαSR[37] (Figures 3c and d) or treated with NF-κB p65-specific siRNAs (Figure 3e) were similarly protected by this pan-sirtuin inhibitor from TNF-induced necroptosis. Cambinol inhibited several early signaling steps known to transduce pro-necroptotic signals in response to TNF including accumulation of phosphorylated JNK (Figure 4a), generation of ROS (Figure 4b) and mitochondrial depolarization (Figure 4c). Finally, cambinol inhibited the assembly of the RIPK1-RIPK3 complex induced by TNF, as assessed by co-immunoprecipitation analysis (Figure 4d). Collectively, these observations indicate that the activity of one or more members of the NAD^+-dependent sirtuin family is required for optimal execution of a necroptotic program.

Both SIRT2 and SIRT5 regulate cell necroptosis. To identify members of the sirtuin family regulating cell survival in response to TNF, a series of lentiviral vectors expressing shRNA directed at all seven sirtuin members was generated and used to infect the L929 cell line. shRNAs to SIRT2 and SIRT5 shown to selectively affect expression of their target gene by both mRNA and protein analysis (Figures 5a and b) and were found to protect cells from TNF-induced necroptosis (Figures 5c and e). Knockdown of both sirtuin members led to a sub-optimal assembly of the RIPK1-RIPK3 complex in response to TNF (Figures 5d and f). To further confirm the role for SIRT5 for adequate response to TNF, L929 cells were transfected with siRNA specific for SIRT1 (used as a negative control), SIRT5 and RIPK3 (used as a positive control) (Figure 5h). A summary of nine independent experiments is shown in Figure 5g, confirming that a weak, albeit statistically significant protection against necroptosis can be achieved upon administration of siRNA to SIRT5. These results were also confirmed in L929 cells invalidated for SIRT2, SIRT5 or both sirtuins using the CRISPR/Cas9 technology (Supplementary Figure S4a and S4c). Again deletion of SIRT2 and SIRT5 conferred a significant protection against TNF-induced necroptosis (Supplementary Figure S4b and S4d). Moreover, invalidation of SIRT2 did not affect the sensitivity of L929 cells to FAS-induced apoptosis (Supplementary Figure S4e).

Sirtuin-dependent regulation of necroptosis requires caspase-8 activity. Much to our surprise, the protective effect of cambinol was found to require caspase activity. Indeed, when L929 cells were treated by a combination of

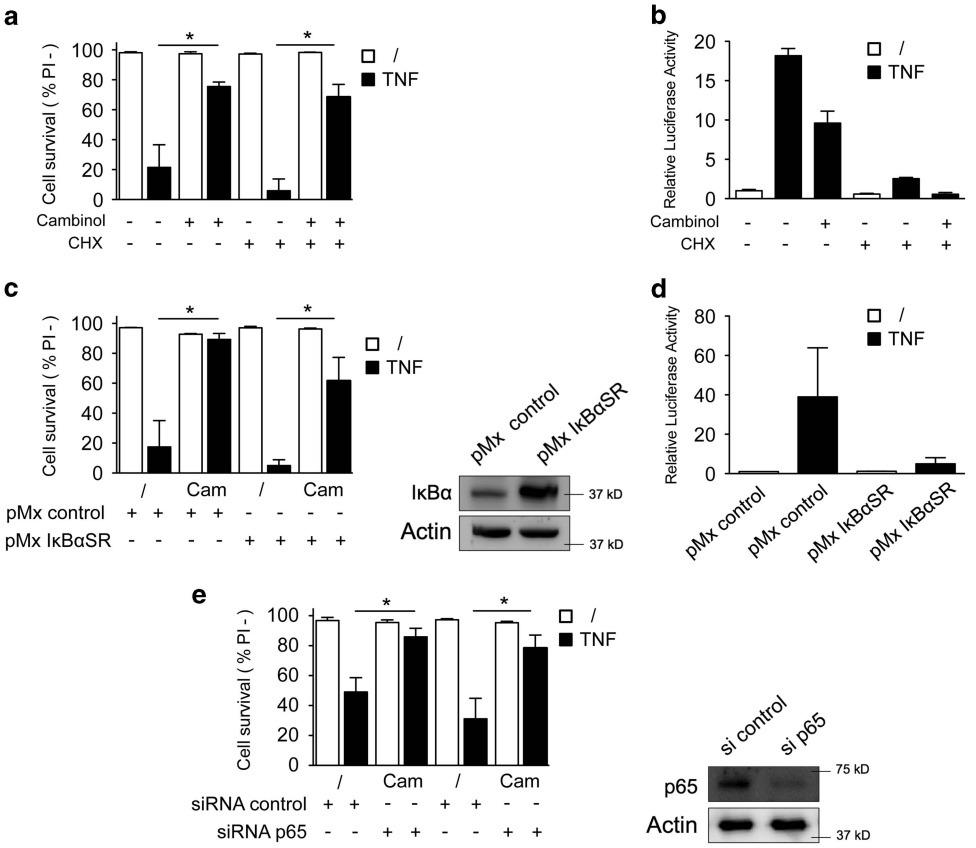

Figure 3 Cambinol protects L929 cells from TNF-induced cell death independently of novel protein synthesis and NF-κB signaling. (**a**) Cell survival in response to recombinant hTNF (1 ng/ml)-induced necroptosis was assessed in L929 cells in the presence of cycloheximide (10 μM) ($n=4$). (**b**) HEK293T cells were transfected with a reporter plasmid expressing luciferase under the control of multiple κB-sites. Cells were stimulated with recombinant hTNF in the presence of cambinol (100 μM) and/or cycloheximide (CHX, 10 μM) ($n=4$). (**c**, **d**) L929 cells were stably transduced with viral constructs coding for the IκBα super repressor (IκBαSR). (**c**) Cell survival in response to recombinant hTNF (1 ng/ml) was assessed 16 h post-treatment in L929 cells expressing IκBαSR in the presence of cambinol (100 μM) ($n=4$). (**d**) Luciferase expression and western blot analysis were used to confirm the inhibitory properties of IκBαSR on NF-κB signaling ($n=4$) and IκBα stability ($n=2$). (**e**) L929 cells transfected with p65 siRNA were incubated in the presence of TNF (1 ng/ml) and cambinol (100 μM) before cell survival analysis after 16 h ($n=4$). The expression of p65 in control and siRNA-treated L929 cells was monitored by western blotting ($n=2$). Data represent mean+SD of four independent experiments (*$P<0.05$)

TNF and the pan-caspase inhibitor z-VAD.fmk, they became resistant to the pro-survival effects of cambinol (Figures 6a–c). As expected, necrostatin-1 protected cells exposed to TNF and z-VAD.fmk, confirming that caspase inhibition favors a necroptotic form of cell death. Similarly, and in contrast to necrostatin-1, cambinol was unable to protect L929 cells from necroptotic cell death induced by FAS signaling in the presence of z-VAD.fmk[21,38] (Figure 6d). Owing to the well-described role for caspase-8 in protecting cells from RIPK3-dependent cell death,[39,40] we next exposed L929 cells to TNF in the presence of z-IETD.fmk, a specific caspase-8 inhibitor. Pharmacological inhibition of caspase-8 impeded cambinol-mediated cell survival, suggesting a possible link between sirtuins and caspase-8 activity in counteracting TNF-induced necroptosis (Figure 6e). To further substantiate these observations, we evaluated the capacity of cambinol to modulate the activity of caspase-8. Using a western blot (Figure 6f) and a caspase-8 fluorogenic assay (Figure 6g), we detected an increased activity of this caspase in cambinol-treated cells exposed to a FAS ligand, but not TNF. Note, however, that the assays used can only reveal the catalytically activity of the pro-apoptotic caspase-8 homodimer, since the pro-survival caspase-8/cFLIP heterodimer does not require processing and displays a distinct substrate repertoire.[41] To further support a role for caspase-8-containing heterodimers in this setting, we stably expressed the viral protein Crma in L929 cells.[42] Contrary to most pharmacological inhibitors, this protein has been shown to preferentially inhibit caspase-8/caspase-8 homodimers over cFLIP/caspase-8 heterodimers, known to negatively regulate necroptosis.[39,43] Cells expressing Crma were strongly sensitized to TNF-induced cell death, while efficiently protected by cambinol (Figure 6h), suggesting that sirtuin inhibitors may exert their anti-necroptotic activities by enhancing the survival properties of cFLIP/caspase-8 heterodimers in response to TNF.

Cambinol protects from renal ischemia/reperfusion injury. Finally, to demonstrate the *in vivo* relevance of these findings, cambinol was assayed in a model of renal ischemia-reperfusion injury (IRI). Necroptosis is indeed thought to have a major pathological role during renal ischemia-reperfusion, based on the organ-preserving properties of necrostatin-1 in animal models[44,45] and the relative resistance of RIPK3-KO

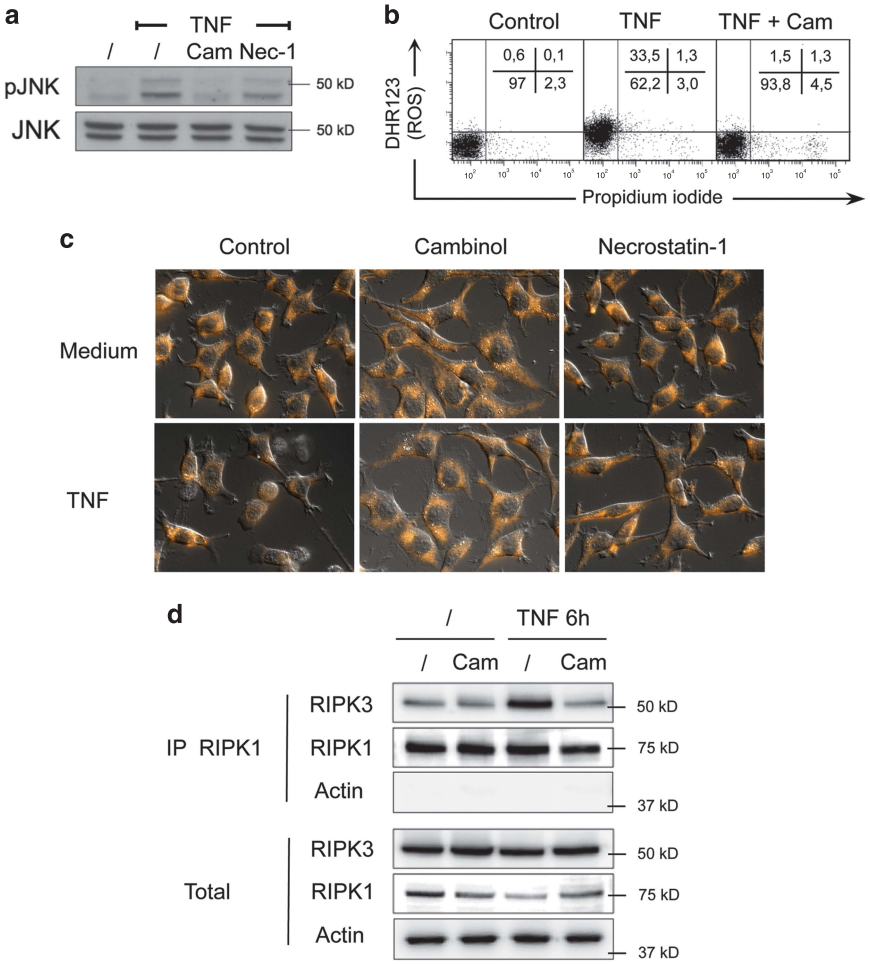

Figure 4 **C**ambinol interferes with the molecular execution of necroptosis. (**a**) Cambinol (100 μM) or necrostatin-1 (20 μM)-treated L929 cells were incubated in the presence of hTNF (1 ng/ml) for 20 min and the phosphorylated status of JNK determined by western blot ($n=3$). (**b**) Flow cytometry analysis of ROS production, assessed as DHR123 fluorescence in TNF-stimulated L929 cells previously exposed to 100 μM cambinol ($n=4$). (**c**) Mitochondrial depolarization of control or drug-treated L929 cells in response to hTNF (1 ng/ml) was estimated after 6 h using TMRE staining ($n=3$). (**d**) Cambinol (100 μM)-treated L929 cells were stimulated with hTNF for 6 h, and cell extracts analyzed for the presence of RIPK1-RIPK3 protein complexes ($n=5$) as indicated in the legend to Figure 1. Data are representative of at least three independent experiments

animals to IRI.[46] IRI was induced by clamping of left renal artery for 20 min followed by 24 h of reperfusion. Necrotic damage was reduced in RIPK3-deficient mice, and virtually absent in contralateral internal control kidney using this IRI protocol. (Figures 7a, b and e), Pretreatment of mice with cambinol 15 min before clamping led to reduced medulla and cortex necrosis (Figures 7c, d and f), compatible with an *in vivo* role for sirtuins in mediating necroptotic damage in response to IRI.

Discussion

The recent recognition of several, often independent, forms of programmed cell death led us to undertake a comparative study examining how the metabolite NAD^+, a putative intracellular pro-survival factor, regulates necroptosis. The observations reported in the present study, and performed primarily using a cell line in which apoptosis and necroptosis could be selectively induced using well-characterized ligands and experimental conditions, unveil a critical role for intracellular NAD^+ in determining the sensitivity of cells to necroptosis. Independently of the experimental strategy used, an increase in intracellular NAD^+ levels sensitized cells to necroptosis, while reduction in NAD^+ levels protected cells against this form of programmed cell death. Intracellular NAD^+ levels were found to affect a relatively proximal step in the necroptotic signaling cascade initiated by the TNFR1, as shown by the reduced capacity of TNF to induce RIPK1-RIPK3 complexes in cells displaying low intracellular NAD^+ levels.

On the basis of the well-described capacity of members of the sirtuin family of NAD^+-dependent deacylases to sense and translate intracellular NAD^+ levels into a biological response, we analyzed the potential role of these enzymes in controlling necroptosis in response to TNF. Use of three structurally unrelated sirtuin inhibitors, including compound 64,[35] the most potent and specific SIRT2 inhibitor described to date, and cambinol, a previously described putative pan-sirtuin inhibitor,[47,48] largely confirmed our working hypothesis, as incubation of cells in the presence of these compounds

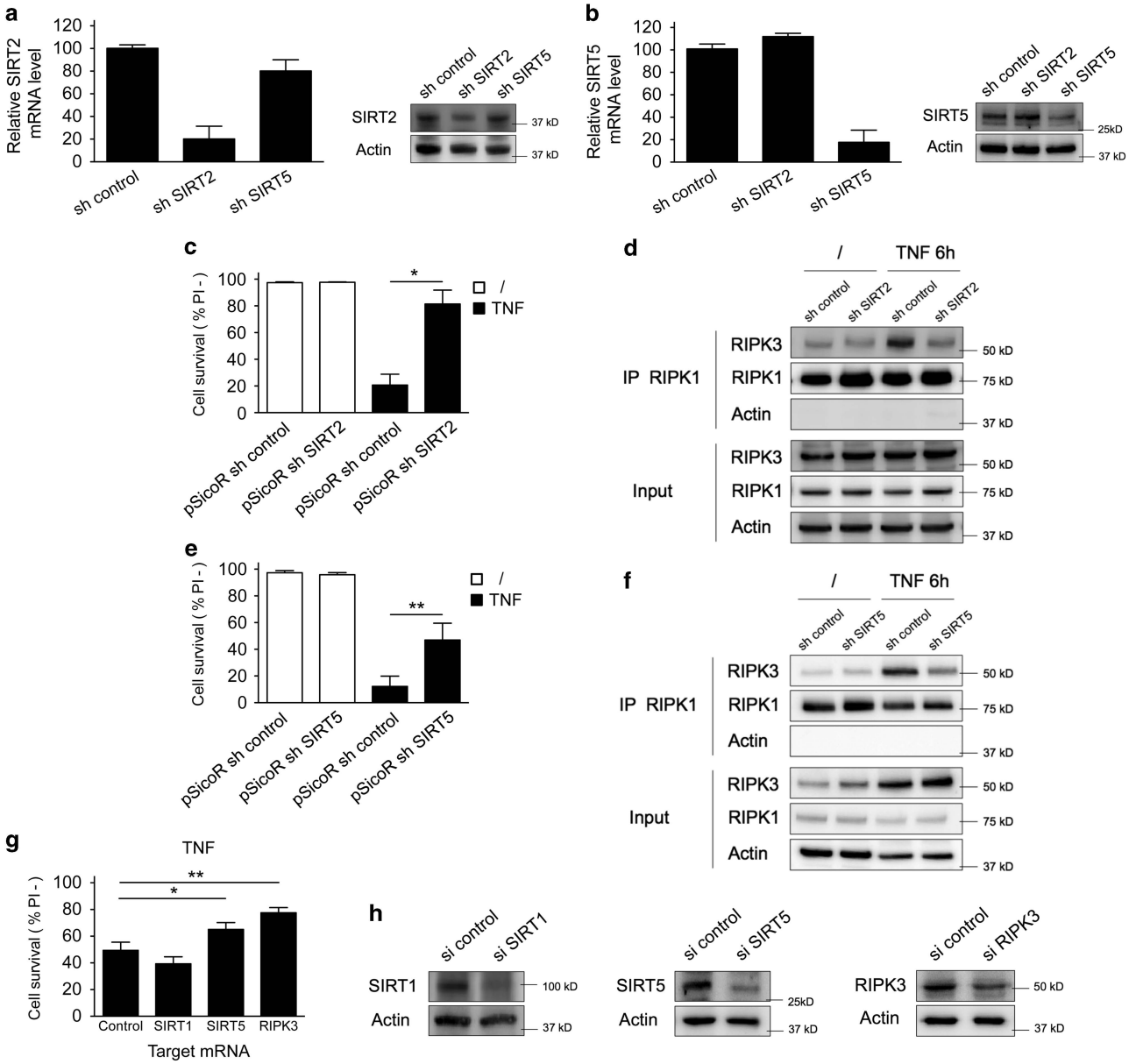

Figure 5 Reduction of SIRT2 and SIRT5 protein levels opposes necroptosis. L929 cells were stably transduced with vectors expressing shRNA constructs targeting SIRT2 (**a**, **c** and **d**) or SIRT5 (**b**, **e** and **f**) as indicated. Efficacy and specificity of each shRNA is illustrated in (**a**) and (**b**), using RT-PCR ($n=3$) and western blot ($n=3$) analysis. (**c**, **e**) L929 were assessed for cell survival in response to recombinant hTNF (1 ng/ml) 16 h post-treatment (shRNA SIRT2 $n=4$; shRNA SIRT5 $n=6$). (**d**, **f**) The presence of RIPK1-RIPK3 complexes was determined as described in Figure 1 ($n=3$). (**g**) L929 cells were treated with siRNA to the indicated proteins, exposed to hTNF and assayed for cell viability as previously described ($n=9$). (**h**) Efficacy and specificity of siRNA treatments were verified by western blot using the appropriate corresponding antibodies. Cell survival graphs represent mean+SD of at least four independent experiments (*$P<0.05$, **$P<0.01$), and western blot graphs are representative of three independent experiments

rescued cells from necroptosis. In keeping with a previous report,[33] a knockdown approach confirmed the requirement for SIRT2 expression and activity to complete the necroptotic program, but also led us to identify SIRT5 as a critical, additional sirtuin member regulating this form of cell death. Both SIRT2 and SIRT5 appeared to affect the stability of RIPK1-RIPK3 association. Whether these two sirtuins share the same substrate (as previously described and discussed for other sirtuins pairs)[49] and/or affect distinct substrates involved in necrosome assembly is presently unknown and under investigation. The present work may help to shed some light on the controversial issue surrounding the role of sirtuins in necroptosis. Indeed, the report describing a role for SIRT2 in promoting necroptosis has been recently challenged by a panel of authors.[50] We believe that our work provides new experimental evidence that may help better apprehend the role of sirtuins in regulating necroptosis. First, we have consistently failed to inhibit necroptosis induced in the presence of a pan-caspase inhibitor by affecting sirtuin activity and/or expression. This observation raises the intriguing possibility that sirtuins may facilitate necroptosis by counter-acting the inhibitory properties of the cell protective

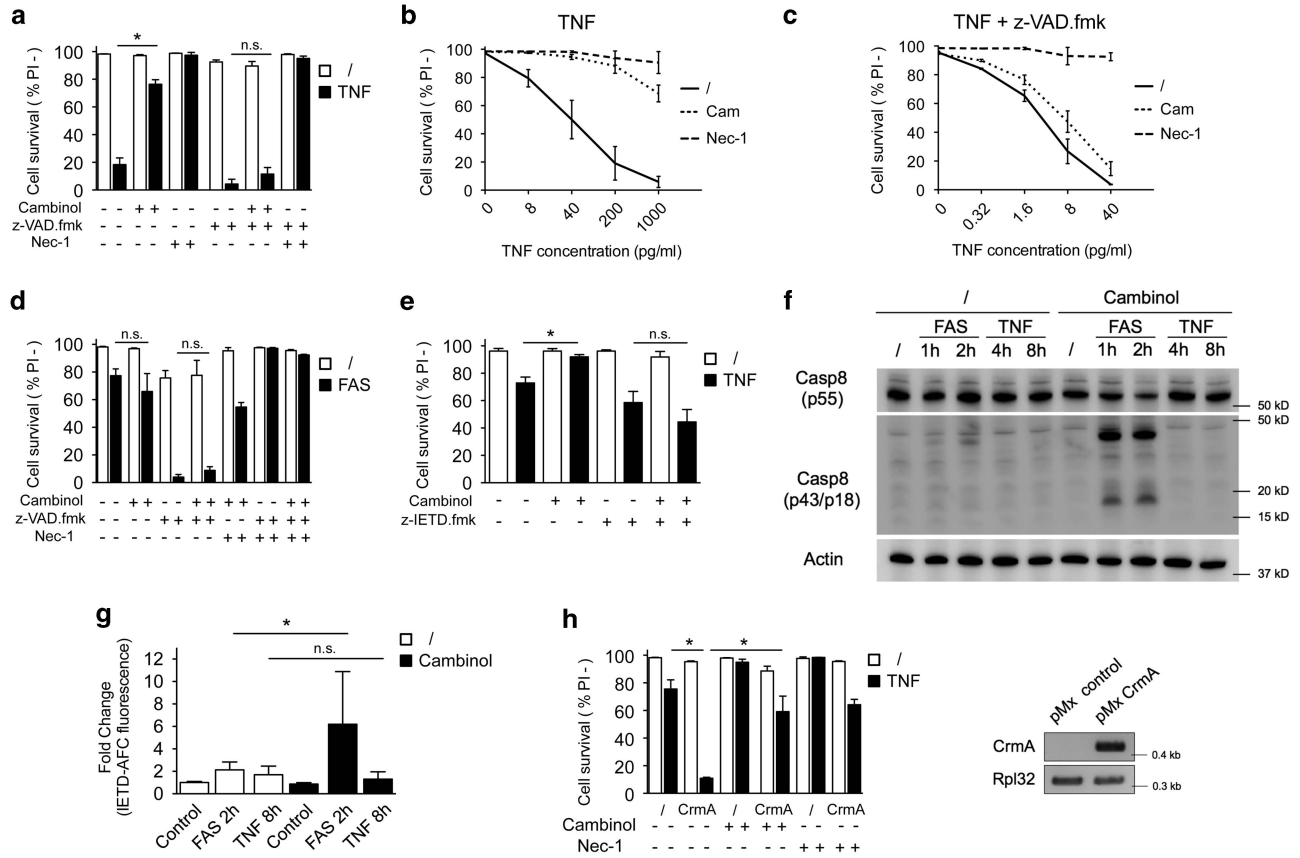

Figure 6 The protective effect of cambinol on necroptosis requires caspase activity. (**a**) Cell survival in response to recombinant hTNF (1 ng/ml)-induced necroptosis was assessed 16 h post-treatment in L929 cells previously incubated in the presence of cambinol (100 μM), necrostatin-1 (20 μM), z-VAD.fmk (25 μM) and combinations of these compounds ($n=4$). (**b**, **c**) Cell survival in response to a combination of graded doses of TNF and cycloheximide (10 μg/ml) was assessed 16 h post-treatment in the absence (**b**), or in the presence (**c**) of z-VAD.fmk (25 μM) and the indicated inhibitors, cambinol (100 μM) and necrostatin-1 (20 μM) ($n=3$). (**d**) Cell survival in response to FAS (CH-11; 15 ng/ml)-induced cell death after 16 h of treatment was assessed in L929 cells previously incubated in the presence of cambinol (100 μM), necrostatin-1 (20 μM), z-VAD.fmk (25 μM) and combinations of these compounds ($n=4$). (**e**) Cell survival in response to recombinant hTNF (200 pg/ml)-induced necroptosis was assessed 16 h post-treatment in L929 cells previously incubated in the presence of cambinol (100 μM), z-IETD.fmk and a combination of both compounds ($n=4$). Caspase-8 activity in response to hTNF (10 ng/ml) and FAS agonist (CH-11; 100 ng/ml) was assessed in the presence of cambinol (100 μM), by (**f**) western blot to detect full length and processed forms of caspase-8 ($n=3$) or, (**g**) using fluorescence emitted by a fluorogenic caspase-8 substrate, IETD-AFC ($n=4$). (**h**) Cell survival in response to recombinant hTNF (200 pg/ml) was assessed at 16 h post-treatment in L929 cells stably expressing CrmA and previously incubated in the presence of cambinol (100 μM) or necrostatin-1 (20 μM) ($n=4$). PCR analysis was used to confirm the expression of CrmA in L929 cells. Data represent mean+SD of four independent experiments (*$P<0.05$)

cFLIP/caspase-8 heterodimer. Although indirect, the capacity of cambinol to promote caspase-8 activity in response to FAS, but not TNF stimulation, in the cell line used in this study is compatible with this working hypothesis that, however, needs further investigation. Of further note, we believe that caution should prevail when studying necroptosis induced in the presence of pan-caspase inhibitors. Indeed, (i) a number of off-targeting effects interfering with necroptosis were reported for caspases inibitors.[51,52] (ii) In addition to masking the potential role of the NAD^+-sirtuin axis, recent observations indicate that these inhibitors can promote the production of soluble factors, including a number of cytokines (IL-6, IL-1β, IL-8, GM-CSF and CXCL2), chemokines (CCL2, RANTES and CXCL1)[53] and type I interferons (in response to mitochondrial damage)[54,55] that could interfere with the necroptotic signaling pathway.[56–58]

Although the present study confirms previously reported observations suggesting a role for SIRT2 in promoting necroptosis,[33] they are at apparent odds with the observation that SIRT2-KO mice remain sensitive to the *in vivo* toxicity of exogenously administered TNF.[50] Possible explanations for this apparent discrepancy include the possible functional redundancy between sirtuin members as this multigene family often share substrate specificity[49] and the uncertainty concerning the mechanism underlying TNF toxicity in SIRT2-KO mice.[50] Also of relevance are the observations that, quite often, inhibition of sirtuin activity can promote an alternative form of cell death (see Figure 2d and Supplementary Figure S3b), warranting further investigations in the mode of cell death induced by TNF in SIRT2-KO mice.[50]

Necrostatin-1 has been found to provide protection against tissue damage secondary to ischemia and reperfusion in several mouse models, strongly suggesting an important role for necroptosis in these pro-inflammatory forms of cell death. The protective role of a sirtuin inhibitor in a model of ischemia-related, RIPK3-dependent, tissue damage (Figure 7) not only confirms the previously described *in vitro* observations, but also expands the possible pharmacological intervention

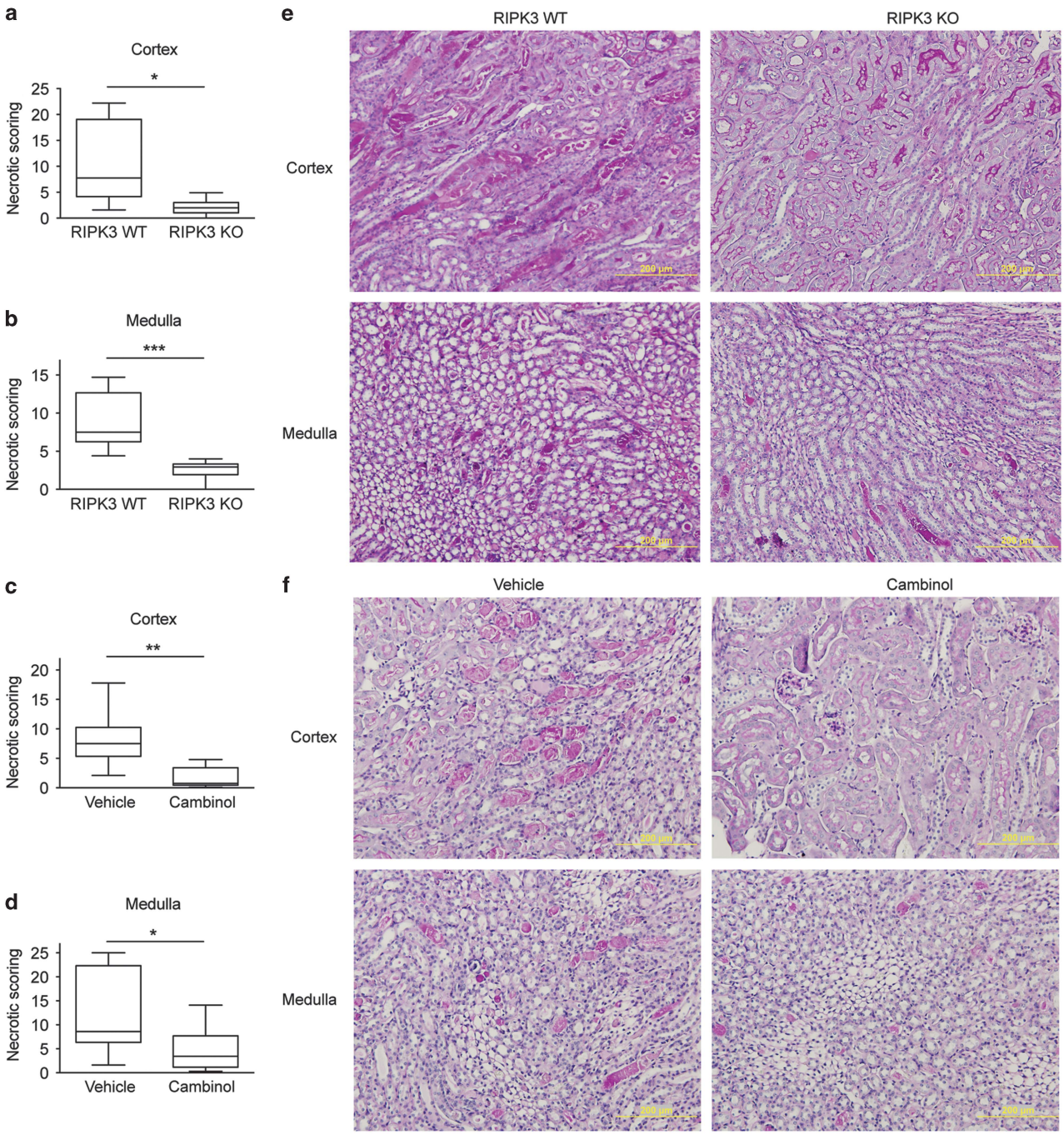

Figure 7 Cambinol protects from renal ischemia/reperfusion injury. Mice were pretreated with cambinol ($n=8$) or vehicle ($n=8$) 15 min before clamping, or simply clamped for RIPK3 WT ($n=6$) and RIPK3-KO mice ($n=8$), and exposed to ischemia/reperfusion. A necrosis scoring was attributed for renal (**a** and **c**) medulla and (**b** and **d**) cortex lesions. (**e** and **f**) Representative pictures of kidney sections stained with periodic acid Schiff after diastase treatment (PAS-d) to identify renal lesions after ischemia/reperfusion at 10 times magnification. Pink/purple staining marks necrotic cells. Data are representative of three independent experiments (*$P<0.05$, **$P<0.01$, ***$P<0.001$)

aimed at protecting tissues from oxidative/inflammatory damages. Notably, it is tempting to speculate that based on the differential sensitivity of necrostatin-1 and cambinol to caspase inhibition, these two compounds may affect distinct signaling steps and could be used in combination for increased clinical benefit.

In conclusion, the present study confirms the important signaling role played by NAD^+ and highlights the complex relationship between metabolism and cell survival. While intracellular NAD^+ protects cells against PARP-1-dependent cell death and possibly also against some forms of apoptosis[59–61] and autophagy,[60,62] it has an opposite role in promoting necroptosis. NAD^+ may therefore represent an important intracellular factor regulating the choice of cell demise, a finding that may call for caution in the clinical translation of pharmacological and nutraceutical approaches

aiming at increasing tissue NAD^+ levels with the hope of counteracting aging-related disabilities.[63]

Materials and Methods

Cell lines and culture media. L929sAhFas cells (referred to as L929 in this study) were generated by expressing the human Fas gene in L929sA cells, a TNF-sensitive derivative of the murine fibrosarcoma cell line L929.[23] Human embryonic kidney (HEK) 293T, L929 and MEF cells were cultured in Dulbecco's modified Eagle's medium (DMEM) supplemented with 10% fetal calf serum (FCS), penicillin (100 IU/ml), streptomycin (0.1 mg/ml) and L-glutamine (0.03%).

Compounds, antibodies and cytokines. Primary antibodies used for western blot were RIPK1 mAb (38/RIP, BD Biosciences, San Jose, CA, USA), RIPK3 pAb (#IMG-5523-2, Imgenex, Littleton, CO, USA), Caspase-8 mAb (1G12, Alexis Biochemicals, Farmingdale, NY, USA); NAMPT mAb (14A.5, Millipore, Billerica, MA, USA), Actin pAb (#A2066), tubulin mAb (B-5-1-2) and acetylated tubulin mAb (6-11B-1) were from Sigma-Aldrich (St. Louis, MO, USA), SIRT5 pAb (#ARP40125_T100, Aviva Systems Biology, San Diego, CA, USA), cleaved caspase-8 mAb (#D5B9) and SIRT2 mAb (#D4S6J) were from Cell Signaling (Danvers, MA, USA) and SIRT1 pAb (#07–131, Millipore). Finally, Vimentin pAb (#SC-7557), p65 pAb (#SC-372), and IκB-α pAb (#SC-371) were from Santa-Cruz Biotechnology (Dallas, TX, USA). Secondary antibodies used for western blot were donkey anti-goat IgG-HRP (#SC-2020, Santa-Cruz Biotechnology), mouse anti-rat kappa chain (clone LO-MK-1, Thermo Scientific, Waltham, MA, USA), donkey anti-rabbit IgG-HRP (#NA934V) and sheep anti-mouse Ig-HRP (#NXA931) were from GE Healthcare (Little Chalfont, UK), and HRP-rec-Protein G (#10–1223) was from Invitrogen (Waltham, MA, USA). Purified mAb raised against human FAS (clone: CH11) was purchased from Millipore. Recombinant murine and human TNF (#315-01A and #300-01A, respectively) were from Peprotech (Rocky Hill, NJ, USA). SIRT1 inhibitor EX-527 (#566322) was from Calbiochem (Billerica, MA, USA). NAMPT inhibitor FK866 is a gift from Apoxis (Lausanne, Switzerland). Staurosporine (#S5921), ionomycin (#I9657), cambinol (#C0494), nicotinamide mononucleotide (#N3501), isonicotinamide (#I17451) were all purchased from Sigma-Aldrich. Necrostatin-1 (#ALX-430-136) was from Alexis Biochemicals, z-VAD.fmk (#3188-v) from Peptanova (Sandhausen, Germany) and z-IETD.fmk (#550380) from BD Pharmingen (San Jose, CA, USA). RIPK3 inhibitor (GSK'843, described here as R3i), a kind gift of GSK was used under an MTA agreement, and requests should be addressed to P.J.G. (peter.j.gough@gsk.com). The SIRT2 inhibitor (compound 64) was kindly provided by Liqiang Chen (University of Minnesota, Minneapolis, USA).

Transfection and RNA interference. Cells were transfected with Lipofectamine 2000 (Invitrogen) following manufacturer's instructions. A GFP reporter plasmid was used to estimate transfection efficacy by flow cytometry. L929 cells were transfected with pools of four distinct proprietary siRNAs (siGENOME SMARTpool, Dharmacon) to each target mRNA at 35 nM using Lipofectamine 2000 as a transfection reagent. As controls, non-targeting siRNA duplexes were employed. Cells were used 48 h post-transfection.

Quantification of NAD. The method used is derived and adapted from a previously described colorimetric test.[64,65] Cells were collected and washed in cold PBS. Cellular pellets were resuspended at about 5×10^7 cells/ml in an extraction buffer containing 20 mM $NaHCO_3$ and 100 mM Na_2CO_3 and snap-frozen in liquid nitrogen. Upon thawing, lysates were centrifuged at 13 000 g for 15 min at 4 °C, and the supernatants collected and stored protected from light on ice. Intracellular NAD quantification relies on an enzymatic cycling assay performed in a 96-well plate. For each sample, 20 μl of cell lysate was mixed with 160 μl of fresh reaction buffer (100 mM Tris-HCl (pH 8.0), 1 mM phenazine ethosulfate (PES, Sigma-Aldrich), 0.5 mM 3-(4,5-dimethylthiazol-2-yl)-2,5-diphenyltetrazolium bromide (MTT, Sigma-Aldrich), alcohol dehydrogenase 0.2 mg/ml et BSA 1%). The enzymatic loop was triggered by adding 20 μl of warm ethanol 6 M and the plate incubated at 37 °C in darkness. Optical density is measured every 3 min for 15 min at 570 nm on a spectrophotometer (Multiscan FC, Thermo Scientific). NAD values are normalized to protein concentrations (Micro BCA Protein Assay kit, Thermo Scientific).

SDS-PAGE and western blot. Cells were lysed in RIPA buffer (PBS with 1% NP-40, 0.5% sodium desoxycholate and 0.1% SDS) containing protease inhibitors (Complete Mini Protease Inhibitor Cocktail Tablet, Roche, Basel, Switzerland). Protein concentration was measured with the Micro BCA Protein Assay kit (Thermo Scientific) and up to 40 μg of protein was loaded onto a 12% Bis-Tris polyacrylamide gel. Gels were run in NuPAGE MOPS or MES SDS Running Buffer (Invitrogen) at 150 V for 1 h. Proteins were transferred onto a PVDF membrane (Amersham, Little Chalfont, UK) with transfer buffer containing 25.5 mM Tris, 192 mM glycine and 20% methanol. Membranes were incubated in 5% BSA or 5% nonfat dry milk (Biorad, #170–6404, Hercules, CA, USA) and proteins were detected with appropriate antibodies. Protein expression was revealed using a Pierce-enhanced chemiluminescence western blotting substrate (ECL) (Thermo Scientific) and recorded on a CCD camera (G:Box Chemi, Syngene, Cambridge, UK).

Immunoprecipitation. Cells were grown overnight in 15 cm dishes. After stimulation, the cells were washed once with PBS and harvested by scraping. After centrifugation at 500 *g* for 5 min at 4 °C, the cell pellet was washed again in cold PBS and resuspended in 1 ml of lysis buffer (50 mM Tris, pH 8.0, 150 mM NaCl, 1 mM EDTA, 1% NP-40, 10% glycerol, 20 mM glycerol b-phosphate, 10 mM NaF, 0.5 mM sodium orthovanadate and cOmplete Mini Protease Inhibitor Cocktail Tablet from Roche) and incubated on an orbital shaker at 4 °C for 15 min. Cell lysates were cleared by centrifugation at 16.000 *g* for 15 min at 4 °C and supernatants incubated overnight with an antibody to RIP1 (clone: 38/RIP, BD Biosciences). The complex was isolated using the μMACS μbeads technology (Miltenyi Botec, Bergisch Gladbach, Germany) following the manufacturer's instructions. In brief, secondary antibody coupled-μbeads were added for 60 min, and cell lysate was applied to a μ-column, washed four times and eluted with 50 μl of pre-heated (95 °C) elution buffer containing two volumes of LAEMLI buffer 5X+ 2% β-mercaptoethanol and three volumes of lysis buffer. The eluate was analyzed by SDS-PAGE.

RNA purification, cDNA synthesis and RT-PCR. Total RNA was extracted from the cells using TRIzol Reagent (Invitrogen). Poly(A) RNA was primed with oligo(dT) (Sigma-Aldrich) and reverse transcribed with SuperScript reverse transcriptase (Roche) for 1 h at 42 °C. To estimate the expression of CrmA, cDNA products were amplified by PCR using primers specific for mouse Rpl32 (5′ primer, 5′-CTG CCC TCC GGC CTC TGG TG-3′; 3′ primer, 5′-GCG TAG CCT GGC GTT GGG AT-3′), cowpow virus CrmA (5′ primer, 5′-ACG GCG AGG CAT TTA ATC ACG CA-3′; 3′ primer, 5′-CAG TCT GCC ACC AGC GCA CA-3′). All primers were purchased from Sigma-Aldrich. To estimate the expression of CrmA, a 50 μl PCR reaction was set up containing 0.4 μl (1 U) of Taq DNA polymerase produced in the laboratory, 5 μl of 10X Red Taq buffer (Sigma-Aldrich), 2 μl of cDNA and 200 nmol of each primer. Amplification consisted of 30 cycles of denaturation at 95 °C for 15 s, annealing at 55 °C for 30 s and extension at 68 °C for 1 min. Amplification products were electrophoresed on 1% agarose gels and visualized by ethidium bromide staining on a CCD camera (G:Box Chemi, Syngene). To estimate shRNA specificity and efficacy, cDNA products were amplified by PCR using primers specific for mouse Rpl32 (5′ primer, 5′–GGC ACC AGT CAG ACC GAT AT–3′; 3′ primer, 5′–CAG GAT CTG GCC CTT GAA C–3′), Sirt2 (5′ primer, 5′-AAC ATC CGG AAC CCT TCT TT-3′; 3′ primer, 5′-AGC AGG CGG ATG AAG TAG TG-3′ and Sirt5 (5′ primer, 5′-CAC CCA GAA CAT TGA CGA GTT-3′; 3′ primer, 5′-TAA GGT TCC GTG GAT TTC CA-3′). qPCR was performed using a StepOne Plus system (Applied Biosystems) with Maxima SYBR Green/ROX qPCR Master Mix (Thermo Fisher Scientific). Quantification (with RPL32 as endogenous housekeeping gene) was done using standard curves.

Cell death analysis and caspase-8 assay. Flow cytometry was used to quantify cell death using a FACS Canto II cytometer (Becton Dickinson, San Jose, CA, USA). Plasma membrane integrity is disrupted in necrotic cells and secondary necrotic cells, allowing propidium iodide incorporation and staining of DNA. Propidium iodide negative cells (PI-) were considered as viable cells. Caspase-8 activity was assessed using IETD substrate peptide conjugated to 7-amino-4-trifluoromethyl coumarin (AFC) following the manufacturer's instructions (R&D Systems, Minneapolis, MN, USA, #BF2100). Fluorescence emitted at 505 nm was measured using Synergy Mx microplate reader (Biotek, Winooski, VT, USA).

TMRE staining. For mitochondrial membrane potential measurements, L929 cells were cultured in chambered coverglass (CELLview, Greiner), washed once with phosphate-buffered saline and stained for 30 min at 37 °C with 100 nM Tetramethylrhodamine ethyl ester (TMRE, Invitrogen). TMRE is a cationic cell permeable red-orange fluorescent dye that is readily sequestered by active mitochondria. Loss of mitochondrial membrane potential cells is detected by attenuation of TMRE fluorescence. Images were captured using an inverted fluorescence microscope (Zeiss Axio Observer Z1) equipped with a thermostated incubation chamber.

ROS detection and analysis. L929 cells were cultured and treated in 24-well plates. For the last 30 min of stimulation, dihydrorhodamine 123 (DHR123, #D-632) from Invitrogen was added in the medium at a concentration of 5 nM. Propidium iodide was added just before flow cytometry analysis.

Luciferase assays. Cell lysis and luciferase assays were performed using the Dual-Luciferase Reporter Assay System (Promega, Fitchburg, WI, USA) following the manufacturer's instructions. The luminescence was measured using a luminometer (TD-20/20, Turner Designs, Sunnyvale, CA, USA). HEK293T cells were transfected with a reporter plasmid in which the firefly luciferase reporter gene is under control of multiple κB-sites from the IL-6 promoter binding sites for the classical p50/p65 dimer.[66] These cells were also transfected with pGL4.74, coding for the Renilla luciferase under control of the constitutive HSV-TK promoter, which serves as an endogenous control.

Mice and *in vivo* experiments. C57BL/6 mice were purchased from Harlan laboratories based in the Netherlands. N.P. holds the Belgian certification to work with laboratory animals. Animal experimentations were conducted in compliance with Belgian and European relevant laws and institutional guidelines. The local ethic committee approved the protocols involving animal experimentation. Renal ischemia reperfusion injury was induced by a 20 min unilateral clamping of the left renal artery, the contralateral kidney was used as an internal control. The surgical procedure was performed under isoflurane anesthesia. After a midline laparotomy, the left renal artery was clamped during 20 min a non-traumatic clamp. Evidence of ischemia was confirmed by the darkening of the ischemic kidney. The abdomen was temporarily closed and body temperature was kept at 36 °C. After removing of the clamp, reperfusion of the kidney was assured by regaining of its original color. The abdomen was closed in two layers and subcutaneous injections with 0.9% NaCl and buprenorfine 50 mg/kg (Temgesic; Schering-Plough) to achieve hydration and analgesia. Cambinol was administered intraperitoneally 15 min before surgery at a dose of 100 mg/kg in a volume of 500 ml. For maximal solubility cambinol was freshly diluted in a solution of 50% ethanol/ 50% cremophore and then mixed with warm PBS to reach a final proportion of 10% ethanol/10% cremophore. Mice were killed 24 h after reperfusion and both kidneys were harvested. Renal tissue was formalin-fixed and paraffin-embedded. Five-μm tissue sections were cut and stained with periodic acid Schiff after diastase treatment to assess necrosis. Necrosis was defined as intraluminal PAS-d+ debris with within denudated tubular basement membranes and necrotic tubules were averaged per $\times$20 high-power field.

Lentiviral and retroviral vectors. Stable expression of proteins of interest was achieved using a modified version of the retroviral vector pMx IRES GFP.[67] The vector was transfected in the Platinum-E (Plat-E) cell line derived from HEK293T cells. Fugene 6 (Promega) was used as a transfection reagent. Stable expression of shRNA targeting proteins of interest was achieved using the lentiviral vector pSicoR eGFP purchased from Addgene (Cambridge, MA, USA). Sequences used were mouse Sirt2 (5′ primer: Tgg aac agc agt aac agt aaT TCA AGA Gat tac tgt tac tgc tgt tcc TTT TTT C; 3′ primer: TCG AGA AAA AAg gaa cag cag taa cag taa TCT CTT GAA tta ctg tta ctg ctg ttc cA) and mouse Sirt5 (5′ primer: Tgt caa gtc ctt cca tat taT TCA AGA Gat aat atg gaa gga ctt gac TTT TTT C; 3′ primer: TCG AGA AAA AAg tca agt cct tcc ata tta TCT CTT GAA taa tat gga agg act tga cA). Lentiviruses were produced following the manufacturer's instructions.

Generation of CRISPR/Cas9-mediated knockout cell lines. L929 cells were transfected with pSpCas9-(BB)2A puro (PX459), a plasmid from Feng Zhang's lab,[68] and knockout cells were selected using puromycin at 10 μg/ml for 5 days. Guide oligos used were mouse Sirt2 (5′ primer: CAC CGG CGG AAG TCA GGG ATA CCC G; 3′ primer: AAA CCG GGT ATC CCT GAC TTC CGC C), and mouse Sirt5 (5′ primer: CAC CGA ACT GGG AAA TGA ATC GGC C; 3′ primer: AAA CGG CCG ATT CAT TTC CCA GTT C).

Statistical analyses. Data presented are expressed as means+SD. Statistical analyses were performed with Mann–Whitney *U*-test (two-tailed distribution) was used for comparison of control group parameters with treatment group, and Kruskal-Wallis was used for multiple comparisons when appropriate. Comparisons of survival curves were performed using Logrank test. Unless specific notification, experiments presented here were reproduced independently at least three times. Difference between groups was considered statistically significant when the *P*-value was below 0.05 ($^*P<0.05$, $^{**}P<0.01$, $^{***}P<0.001$). All statistical analyses were performed with GraphPad Prism5 software (GraphPad Software, San Diego, CA, USA).

Conflict of Interest

NP and OL have recently filed a patent pertaining to the use of isonicotinamide *in vivo*. JB and PJG are employees of GlaxoSmithKline.

Acknowledgements. We thank Iain Welsby and Muriel Moser for reviewing the manuscript and providing helpful suggestions. We wish to acknowledge the support of the Belgian Program in Interuniversity Poles of Attraction initiated by Science Policy Programming, Belgium, the Research Concerted Action and the 'Fonds pour la formation à la Recherche dans l'Industrie et l'Agriculture' (F.R.I.A.) of the 'Fédération Wallonie-Bruxelles', the 'Fonds David et Alice Van Buuren', and the 'Fonds Brachet' for financial support. We wish to thank Adrian Ting (Mount Sinai School of Medicine, NY, USA) and Christine Hawkins (La Trobe University, Victoria, Australia) for sharing plasmids encoding respectively for IκBαSR and CrmA. We also wish to thank Vishva M. Dixit (Genentech, South San Francisco, CA, USA) for sharing RIPK3-KO mice.

Author contributions

Conceived and designed the experiments: NP, OL; performed the experiments and analyzed the data: NP; performed ischemia/reperfusion experiment: MR, JK; analyzed ischemia/reperfusion experiment: JK; contributed reagents/materials/analysis tools: LC, JB, PG, FVG, AR, AL; wrote the paper: OL, NP.

1. Imai S, Guarente L. Ten years of NAD-dependent SIR2 family deacetylases: implications for metabolic diseases. *Trends Pharmacol Sci* 2010; **31**: 212–220.
2. Houtkooper RH, Cantó C, Wanders RJ, Auwerx J. The secret life of NAD+: an old metabolite controlling new metabolic signaling pathways. *Endocr Rev* 2010; **31**: 194–223.
3. Chiarugi A, Dölle C, Felici R, Ziegler M. The NAD metabolome—a key determinant of cancer cell biology. *Nat Rev Cancer* 2012; **12**: 741–752.
4. Feldman JL, Baeza J, Denu JM. Activation of the protein deacetylase SIRT6 by long-chain fatty acids and widespread deacylation by mammalian sirtuins. *J Biol Chem* 2013; **288**: 31350–31356.
5. Verdin E. The many faces of sirtuins: Coupling of NAD metabolism, sirtuins and lifespan. *Nat Med* 2014; **20**: 25–27.
6. Kolthur-Seetharam U, Dantzer F, McBurney MW, de Murcia G, Sassone-Corsi P. Control of AIF-mediated cell death by the functional interplay of SIRT1 and PARP-1 in response to DNA damage. *Cell Cycle* 2006; **5**: 873–877.
7. Alano CC, Garnier P, Ying W, Higashi Y, Kauppinen TM, Swanson RA. NAD+ depletion is necessary and sufficient for poly(ADP-ribose) polymerase-1-mediated neuronal death. *J Neurosci* 2010; **30**: 2967–2978.
8. Yu S-W, Wang H, Poitras MF, Coombs C, Bowers WJ, Federoff HJ *et al.* Mediation of poly (ADP-ribose) polymerase-1-dependent cell death by apoptosis-inducing factor. *Science* 2002; **297**: 259–263.
9. Andrabi Sa, Kim NS, Yu S-W, Wang H, Koh DW, Sasaki M *et al.* Poly(ADP-ribose) (PAR) polymer is a death signal. *Proc Natl Acad Sci USA* 2006; **103**: 18308–18313.
10. Yu S-W, Andrabi Sa, Wang H, Kim NS, Poirier GG, Dawson TM *et al.* Apoptosis-inducing factor mediates poly(ADP-ribose) (PAR) polymer-induced cell death. *Proc Natl Acad Sci USA* 2006; **103**: 18314–18319.
11. Artus C, Boujrad H, Bouharrour A, Brunelle M-N, Hoos S, Yuste VJ *et al.* AIF promotes chromatinolysis and caspase-independent programmed necrosis by interacting with histone H2AX. *EMBO J* 2010; **29**: 1585–1599.
12. Welsby I, Hutin D, Leo O. Complex roles of members of the ADP-ribosyl transferase super family in immune defences: looking beyond PARP1. *Biochem Pharmacol* 2012; **84**: 11–20.
13. Ying W, Garnier P, Swanson RA. NAD+ repletion prevents PARP-1-induced glycolytic blockade and cell death in cultured mouse astrocytes. *Biochem Biophys Res Commun* 2003; **308**: 809–813.
14. Pillai JB, Isbatan A, Imai S, Gupta MP. Poly(ADP-ribose) polymerase-1-dependent cardiac myocyte cell death during heart failure is mediated by NAD+ depletion and reduced Sir2alpha deacetylase activity. *J Biol Chem* 2005; **280**: 43121–43130.
15. Zhu K, Swanson RA, Ying W. NADH can enter into astrocytes and block poly(ADP-ribose) polymerase-1-mediated astrocyte death. *Neuroreport* 2005; **16**: 1209–1212.
16. Yang H, Yang T, Baur Ja, Perez E, Matsui T, Carmona JJ *et al.* Nutrient-sensitive mitochondrial NAD+ levels dictate cell survival. *Cell* 2007; **130**: 1095–1107.
17. Van der Veer E, Ho C, O'Neil C, Barbosa N, Scott R, Cregan SP *et al.* Extension of human cell lifespan by nicotinamide phosphoribosyltransferase. *J Biol Chem* 2007; **282**: 10841–10845.
18. Rongvaux A, Galli M, Denanglaire S, Van Gool F, Drèze PL, Szpirer C *et al.* Nicotinamide phosphoribosyl transferase/pre-B cell colony-enhancing factor/visfatin is required for lymphocyte development and cellular resistance to genotoxic stress. *J Immunol* 2008; **181**: 4685–4695.

19. Rongvaux A, Shea RJ, Mulks MH, Gigot D, Urbain J, Leo O *et al.* Pre-B-cell colony-enhancing factor, whose expression is up-regulated in activated lymphocytes, is a nicotinamide phosphoribosyltransferase, a cytosolic enzyme involved in NAD biosynthesis. *Eur J Immunol* 2002; **32**: 3225–3234.
20. Revollo JR, Körner A, Mills KF, Satoh A, Wang T, Garten A *et al.* Nampt/PBEF/Visfatin regulates insulin secretion in beta cells as a systemic NAD biosynthetic enzyme. *Cell Metab* 2007; **6**: 363–375.
21. Holler N, Zaru R, Micheau O, Thome M, Attinger A, Valitutti S *et al.* Fas triggers an alternative, caspase-8-independent cell death pathway using the kinase RIP as effector molecule. *Nat Immunol* 2000; **1**: 489–495.
22. Degterev A, Huang Z, Boyce M, Li Y, Jagtap P, Mizushima N *et al.* Chemical inhibitor of nonapoptotic cell death with therapeutic potential for ischemic brain injury. *Nat Chem Biol* 2005; **1**: 112–119.
23. Vercammen D, Vandenabeele P, Beyaert R, Declercq W, Fiers W. Tumour necrosis factor-induced necrosis versus anti-Fas-induced apoptosis in L929 cells. *Cytokine* 1997; **9**: 801–808.
24. Van Horssen R, Willemse M, Haeger A, Attanasio F, Güneri T, Schwab A *et al.* Intracellular NAD(H) levels control motility and invasion of glioma cells. *Cell Mol Life Sci* 2013; **70**: 2175–2190.
25. McClure JM, Wierman MB, Maqani N, Smith JS. Isonicotinamide enhances Sir2 protein-mediated silencing and longevity in yeast by raising intracellular NAD+ concentration. *J Biol Chem* 2012; **287**: 20957–20966.
26. Degterev A, Maki JL, Yuan J. Activity and specificity of necrostatin-1, small-molecule inhibitor of RIP1 kinase. *Cell Death Differ* 2013; **20**: 366.
27. Li J-X, Feng J-M, Wang Y, Li X-H, Chen X-X, Su Y *et al.* The B-Raf(V600E) inhibitor dabrafenib selectively inhibits RIP3 and alleviates acetaminophen-induced liver injury. *Cell Death Dis* 2014; **5**: e1278.
28. Wang Z, Jiang H, Chen S, Du F, Wang X. The mitochondrial phosphatase PGAM5 functions at the covergence point of multiple necrotic death pathways. *Cell* 2012; **148**: 228–243.
29. Tait SWG, Oberst A, Quarato G, Milasta S, Haller M, Wang R *et al.* Widespread mitochondrial depletion via mitophagy does not compromise necroptosis. *Cell Rep* 2013; **5**: 878–885.
30. Cai Z, Jitkaew S, Zhao J, Chiang H-C, Choksi S, Liu J *et al.* Plasma membrane translocation of trimerized MLKL protein is required for TNF-induced necroptosis. *Nat Cell Biol* 2014; **16**: 55–65.
31. Chen X, Li W, Ren J, Huang D, He W-T, Song Y *et al.* Translocation of mixed lineage kinase domain-like protein to plasma membrane leads to necrotic cell death. *Cell Res* 2014; **24**: 105–121.
32. Mouchiroud L, Houtkooper RH, Auwerx J. NAD^+ metabolism: a therapeutic target for age-related metabolic disease. *Crit Rev Biochem Mol Biol* 2013; **48**: 397–408.
33. Narayan N, Lee IH, Borenstein R, Sun J, Wong R, Tong G *et al.* The NAD-dependent deacetylase SIRT2 is required for programmed necrosis. *Nature* 2012; **492**: 199–204.
34. Solomon JM, Pasupuleti R, Xu L, McDonagh T, Curtis R, DiStefano PS *et al.* Inhibition of SIRT1 catalytic activity increases p53 acetylation but does not alter cell survival following DNA damage. *Mol Cell Biol* 2006; **26**: 28–38.
35. Cui H, Kamal Z, Ai T, Xu Y, More SS, Wilson DJ *et al.* Discovery of potent and selective sirtuin 2 (SIRT2) inhibitors using a fragment-based approach. *J Med Chem* 2014; **57**: 8340–8357.
36. Heltweg B, Gatbonton T, Schuler AD, Posakony J, Li H, Goehle S *et al.* Antitumor activity of a small-molecule inhibitor of human silent information regulator 2 enzymes. *Cancer Res* 2006; **66**: 4368–4377.
37. Legarda-Addison D, Hase H, O'Donnell Ma, Ting aT. NEMO/IKKgamma regulates an early NF-kappaB-independent cell-death checkpoint during TNF signaling. *Cell Death Differ* 2009; **16**: 1279–1288.
38. Hitomi J, Christofferson DE, Ng A, Yao J, Degterev A, Xavier RJ *et al.* Identification of a molecular signaling network that regulates a cellular necrotic cell death pathway. *Cell* 2008; **135**: 1311–1323.
39. Oberst A, Dillon CP, Weinlich R, McCormick LL, Fitzgerald P, Pop C *et al.* Catalytic activity of the caspase-8-FLIP(L) complex inhibits RIPK3-dependent necrosis. *Nature* 2011; **471**: 363–367.
40. Kaiser WJ, Upton JW, Long AB, Livingston-Rosanoff D, Daley-Bauer LP, Hakem R *et al.* RIP3 mediates the embryonic lethality of caspase-8-deficient mice. *Nature* 2011; **471**: 368–372.
41. Pop C, Oberst A, Drag M, Van Raam BJ, Riedl SJ, Green DR *et al.* FLIP(L) induces caspase 8 activity in the absence of interdomain caspase 8 cleavage and alters substrate specificity. *Biochem J* 2011; **433**: 447–457.
42. Lovric MM, Hawkins CJ. TRAIL treatment provokes mutations in surviving cells. *Oncogene* 2010; **29**: 5048–5060.
43. O'Donnell MA, Perez-Jimenez E, Oberst A, Ng A, Massoumi R, Xavier R *et al.* Caspase 8 inhibits programmed necrosis by processing CYLD. *Nat Cell Biol* 2011; **13**: 1437–1442.
44. Rosenbaum DM, Degterev A, David J, Rosenbaum PS, Roth S, Grotta JC *et al.* Necroptosis, a novel form of caspase-independent cell death, contributes to neuronal damage in a retinal ischemia-reperfusion injury model. *J Neurosci Res* 2010; **88**: 1569–1576.
45. Linkermann A, Bräsen JH, Himmerkus N, Liu S, Huber TB, Kunzendorf U *et al.* Rip1 (receptor-interacting protein kinase 1) mediates necroptosis and contributes to renal ischemia/reperfusion injury. *Kidney Int* 2012; **81**: 751–761.
46. Linkermann A, Bräsen JH, Darding M, Jin MK, Sanz AB, Heller J-O *et al.* Two independent pathways of regulated necrosis mediate ischemia-reperfusion injury. *Proc Natl Acad Sci USA* 2013; **110**: 12024–12029.
47. Lugrin J, Ciarlo E, Santos A, Grandmaison G, dos Santos I, Le Roy D *et al.* The sirtuin inhibitor cambinol impairs MAPK signaling, inhibits inflammatory and innate immune responses and protects from septic shock. *Biochim Biophys Acta* 2013; **1833**: 1498–1510.
48. Maurer B, Rumpf T, Scharfe M, Stolfa Da, Schmitt ML, He W *et al.* Inhibitors of the NAD (+)-dependent protein desuccinylase and demalonylase Sirt5. *ACS Med Chem Lett* 2012; **3**: 1050–1053.
49. Preyat N, Leo O. Sirtuin deacylases: a molecular link between metabolism and immunity. *J Leukoc Biol* 2013; **93**: 669–680.
50. Newton K, Hildebrand JM, Shen Z, Rodriguez D, Alvarez-Diaz S, Petersen S *et al.* Is SIRT2 required for necroptosis? *Nature* 2014; **506**: E4–E6.
51. Temkin V, Huang Q, Liu H, Osada H, Pope RM. Inhibition of ADP/ATP exchange in receptor-interacting protein-mediated necrosis. *Mol Cell Biol* 2006; **26**: 2215–2225.
52. Wu Y-T, Tan H-L, Huang Q, Sun X-J, Zhu X, Shen H-M. zVAD-induced necroptosis in L929 cells depends on autocrine production of TNFα mediated by the PKC-MAPKs-AP-1 pathway. *Cell Death Differ* 2011; **18**: 26–37.
53. Kearney CJ, Cullen SP, Tynan Ga, Henry CM, Clancy D, Lavelle EC *et al.* Necroptosis suppresses inflammation via termination of TNF- or LPS-induced cytokine and chemokine production. *Cell Death Differ* 2015; **22**: 1313–1327.
54. Rongvaux A, Jackson R, Harman CCD, Li T, West AP, de Zoete MR *et al.* Apoptotic caspases prevent the induction of type I interferons by mitochondrial DNA. *Cell* 2014; **159**: 1563–1577.
55. White MJ, McArthur K, Metcalf D, Lane RM, Cambier JC, Herold MJ *et al.* Apoptotic caspases supress mtDNA-induced STING-mediated type I IFN production. *Cell* 2014; **159**: 1549–1562.
56. Robinson N, McComb S, Mulligan R, Dudani R, Krishnan L, Sad S. Type I interferon induces necroptosis in macrophages during infection with Salmonella enterica serovar Typhimurium. *Nat Immunol* 2012; **13**: 954–962.
57. Dillon CP, Weinlich R, Rodriguez DA, Cripps JG, Quarato G, Gurung P *et al.* RIPK1 blocks early postnatal lethality mediated by caspase-8 and RIPK3. *Cell* 2014; **157**: 1189–1202.
58. Günther C, Buchen B, He G-W, Hornef M, Torow N, Neumann H *et al.* Caspase-8 controls the gut response to microbial challenges by Tnf-α-dependent and independent pathways. *Gut* 2014; **64**: 601–610.
59. Hsu C-P, Oka S, Shao D, Hariharan N, Sadoshima J. Nicotinamide phosphoribosyltransferase regulates cell survival through NAD+ synthesis in cardiac myocytes. *Circ Res* 2009; **105**: 481–491.
60. Cea M, Cagnetta A, Fulciniti M, Tai Y-T, Hideshima T, Chauhan D *et al.* Targeting NAD+ salvage pathway induces autophagy in multiple myeloma cells via mTORC1 and extracellular signal-regulated kinase (ERK1/2) inhibition. *Blood* 2012; **120**: 3519–3529.
61. Cagnetta A, Cea M, Calimeri T, Acharya C, Fulciniti M, Tai Y-T *et al.* Intracellular NAD^+ depletion enhances bortezomib-induced anti-myeloma activity. *Blood* 2013; **122**: 1243–1255.
62. Billington RA, Genazzani AA, Travelli C, Condorelli F. NAD depletion by FK866 induces autophagy. *Autophagy* 2008; **4**: 385–387.
63. Gomes AP, Price NL, Ling AJY, Moslehi JJ, Montgomery MK, Rajman L *et al.* Declining NAD (+) induces a pseudohypoxic state disrupting nuclear-mitochondrial communication during aging. *Cell* 2013; **155**: 1624–1638.
64. Zerez CR, Lee SJ, Tanaka KR. Spectrophotometric determination of oxidized and reduced pyridine nucleotides in erythrocytes using a single extraction procedure. *Anal Biochem* 1987; **164**: 367–373.
65. Wagner TC, Scott MD. Single extraction method for the spectrophotometric quantification of oxidized and reduced pyridine nucleotides in erythrocytes. *Anal Biochem* 1994; **222**: 417–426.
66. Plaisance S, Vanden Berghe W, Boone E, Fiers W, Haegeman G. Recombination signal sequence binding protein Jkappa is constitutively bound to the NF-kappaB site of the interleukin-6 promoter and acts as a negative regulatory factor. *Mol Cell Biol* 1997; **17**: 3733–3743.
67. Liu X, Constantinescu SN, Sun Y, Bogan JS, Hirsch D, Weinberg RA *et al.* Generation of mammalian cells stably expressing multiple genes at predetermined levels. *Anal Biochem* 2000; **280**: 20–28.
68. Ran FA, Hsu PD, Wright J, Agarwala V, Scott Da, Zhang F. Genome engineering using the CRISPR-Cas9 system. *Nat Protoc* 2013; **8**: 2281–2308.

Supplementary Information accompanies this paper on Cell Death and Differentiation website (http://www.nature.com/cdd)